All-optical trion generation in single walled carbon nanotubes

Silvia Santos, Bertrand Yuma, Stéphane Berciaud, Jonah Shaver, Mathieu Gallart, Pierre Gilliot, Laurent Cognet, Brahim Lounis

All-Optical Trion Generation in Single-Walled Carbon Nanotubes

Silvia M. Santos,[1] Bertrand Yuma,[2] Stéphane Berciaud,[2] Jonah Shaver,[1] Mathieu Gallart,[2] Pierre Gilliot,[2] Laurent Cognet,[1] and Brahim Lounis[1,*]

[1]*LP2N, Université de Bordeaux, Institut d'Optique and CNRS, 351 cours de la libération, 33405 Talence, France*
[2]*IPCMS, UMR 7504, CNRS–Université de Strasbourg, 23, rue du Læss, 67034 Strasbourg, France*

(Received 4 June 2011; published 27 October 2011)

We present evidence of all-optical trion generation and emission in pristine single-walled carbon nanotubes (SWCNTs). Luminescence spectra, recorded on individual SWCNTs over a large cw excitation intensity range, show trion emission peaks redshifted with respect to the bright exciton peak. Clear chirality dependence is observed for 22 separate SWCNT species, allowing for determination of electron-hole exchange interaction and trion binding energy contributions. Luminescence data together with ultrafast pump-probe experiments on chirality-sorted bulk samples suggest that exciton-exciton annihilation processes generate dissociated carriers that allow for trion creation upon a subsequent photon absorption event.

DOI: 10.1103/PhysRevLett.107.187401 PACS numbers: 78.67.Ch, 71.35.Pq, 78.40.Ri, 78.55.Kz

The optical properties of semiconducting single-walled carbon nanotubes (SWCNTs) are dominated by tightly bound excitons [1,2]. The lowest lying optically active excitons, which dominate the luminescence spectra, have attracted much experimental and theoretical attention over the past decade [3]. Exciton dynamics, and hence nanotube luminescence intensity, are extremely sensitive to the local environment and the presence of quenching sites or structural defects [4,5]. Such extrinsic effects are thought to be responsible for the fairly short luminescence lifetimes (100 ps or less [4,6]) and low luminescence quantum yields reported for individual SWCNTs [6,7].

In the high excitation regime, two or more excitons can be present and their interaction can lead to two different situations. On one hand, they can undergo exciton-exciton annihilation (EEA), which opens up additional, efficient nonradiative recombination pathways [8,9]. On the other hand, excitons may form a biexciton whose stability remains, however, a matter of debate [10–12]. Charged excitons, or trions, are another class of many-body bound states predicted to possess a significant binding energy in SWCNTs [13]. Very recently, Matsunaga *et al.* [14] observed new spectral features in *p*-doped nanotube suspensions assigned to hole-exciton bound states (positively charged trions).

Here we show that trions can be efficiently generated, on demand and *in situ*, in highly luminescent undoped carbon nanotubes through control of photoexcitation intensity. Trion emission below the main exciton peaks of individual SWCNTs, belonging to 22 different chiralities, is observed. A transient absorption feature is recorded at the trion spectral position in pump-probe spectroscopy experiments on a chirality-sorted (6,5) SWCNT suspension. Both luminescence and transient absorption data support a scenario in which localized trions are formed.

For single molecule studies, high pressure (HiPco) SWCNTs were dispersed in sodium deoxycholate solutions and then either immobilized in agarose gels or spin coated on surfaces precoated with polyvinylpyrrolidone. Control experiments on SWCNTs in different surfactants (cetyltrimethylammonium bromide, sodium dodecylbenzene sulfonate, or pluoronic) were performed with similar results. For pump-probe experiments, we used a solution of nonlinear density gradient ultracentrifugation (DGU) sorted (6,5) nanotubes suspended in sodium cholate [15].

SWCNTs were optically excited with tunable cw lasers tuned near their second order resonance S_{22} or at their K-momentum exciton-phonon sideband [16,17]. Individual SWCNTs were imaged with an InGaAs camera and their luminescence spectra were recorded with a spectrometer equipped with an InGaAs detector array. These nanotubes showed stable bright emission with the longest luminescence decays reported to date, signifying low defect density and reduced environmental perturbations [18].

Luminescence spectra of bright individual SWCNTs [inset of Fig. 1(a)] were recorded at low excitation intensities ($\ll 1$ kW/cm^2) in the monoexcitonic regime [Figs. 1(a)–1(c)]. In addition to the bright singlet-exciton peak (X), the phonon sideband of the K-momentum dark exciton is clearly visible at a nearly chirality independent shift of $\sim$130 meV [17,19]. At higher excitation intensities ($>$ kW/cm^2) [Figs. 1(d)–1(f)], a new emission peak (denoted X^*) is systematically observed redshifted with respect to the X peak. However, unlike the phonon sideband, the energy shift ΔE between X and X^* exhibits a strong chirality dependence. The X^* peaks are distinctively redshifted by at least 50 meV as compared to those observed in defect-induced brightening of dark triplet excitons [19–21], and their energies differ significantly from the values observed in oxygen doped SWCNTs [22]. Furthermore, X^* emission appears only at high laser

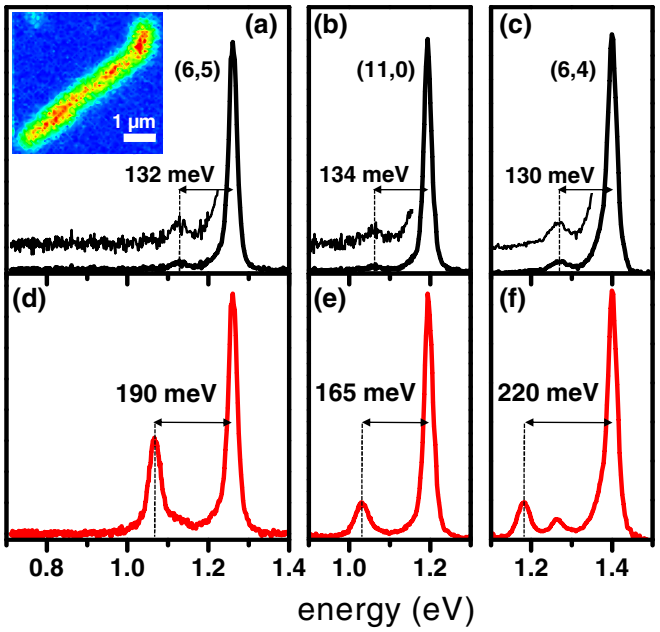

FIG. 1 (color online). Luminescence spectra of bright individual SWCNTs of different chiralities recorded at low cw excitation intensities (a)–(c). Regions of the spectra are expended in order to highlight the K-momentum exciton-phonon sidebands. (Inset: Luminescence image of a typical uniformly bright nanotube). (d)–(f) Luminescence spectra of the same nanotubes as in (a)–(c) recorded under high cw excitation intensities showing new chirality dependent X^* lines.

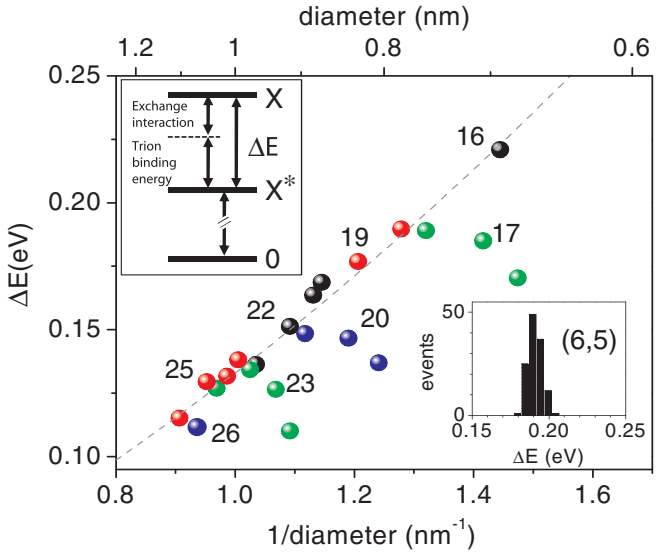

FIG. 2 (color online). Chirality dependence of ΔE. Nanotubes belonging to the same $(2n + m)$ families are displayed with the same colors. The dashed curve is a fit of the near armchair nanotubes with $A/d + B/d^2$ (see text and upper inset). Lower inset: ΔE values obtained from 125 (6,5) nanotubes.

intensities and is absent when returning to the low excitation regime, whereas emission from brightened triplet excitons or oxygen doped SWCNTs is observed at any laser intensity following strong pulsed-laser irradiation [19–21] or exposure to ozone [22].

Single nanotube detection allows determining ΔE's dependence on chiralities with high accuracy (Fig. 2). Each point of Fig. 2 represents the peak value of the ΔE distribution for a given chirality (as exemplified in the inset of Fig. 2). The distributions contained more than a hundred individual SWCNTs for the most abundant chiralities and at least five for minority species. ΔE tends to increase with decreasing SWCNT diameter and displays a clear family pattern. For a given $(2n + m)$ family, deviations from a main trend increase as chiral angle decreases (armchair to zigzag) and are much more pronounced for the $[\mathrm{mod}(n - m, 3) = 1]$ families. This family pattern strongly suggests that the X^* peak stems from an intrinsic property of SWCNTs, and, as they are at the same energies as in Ref. [14], we assign them to trions. In contrast to Matsunaga *et al.*, however, no chemical doping is involved in our study, the carriers being photogenerated on demand in highly luminescent undoped nanotubes allowing their observation on pristine individual nanotubes.

Trion binding energy in SWCNTs is predicted to scale as $1/d$ (d being the tube diameter) and to range, for (6,5) nanotubes, between 50 and 132 meV [13] depending on dielectric screening ($\varepsilon = 4$ and 2, respectively). Here, ΔE is found to be significantly larger [~ 190 meV for (6,5) nanotubes] than the predicted range of ΔE assuming reasonable values of ε for surfactant-wrapped SWCNTs in aqueous environments. Moreover, the diameter dependence of ΔE for near armchair SWCNTs cannot be fitted with an A/d function, as would be expected for a trion formed from a hole and a singlet exciton [13]. Assuming that ΔE includes a contribution from exchange interaction, an additional term is needed. A $1/d^2$ scaling has been predicted for the singlet-triplet splitting that arises due to the exchange interaction [23]. Indeed, we found that a $A/d + B/d^2$ functional form captures the diameter dependence of ΔE (see Fig. 2), suggesting ΔE contains a contribution from the singlet-triplet exciton splitting in addition to the trion binding energy. The fitted trion binding energy constant, $A = 85$ meV $\cdot$ nm, is consistent with a dielectric constant of 2.2 according to Ref. [13], close to that experienced by nanotubes in our experiment. The fitted exchange interaction constant, $B = 48$ meV $\cdot$ nm^2, is in agreement with the theoretical value [23]. Furthermore, as expected, this B value for surfactant-wrapped nanotubes is lower than previously deduced from triplet brightening experiments performed on suspended nanotubes, the latter experiencing lower dielectric screening [14,21].

To investigate the mechanism leading to trion emission, we studied the laser intensity dependence of X and X^* in individual (6,5) SWCNTs (Fig. 3). Distinct segments (~ 0.4–0.5 μm long) of the same bright long nanotubes, a few micrometers away from one another, were used to perform intensity dependent studies at different photon energies. SWCNTs were excited either at 2.21 eV, near

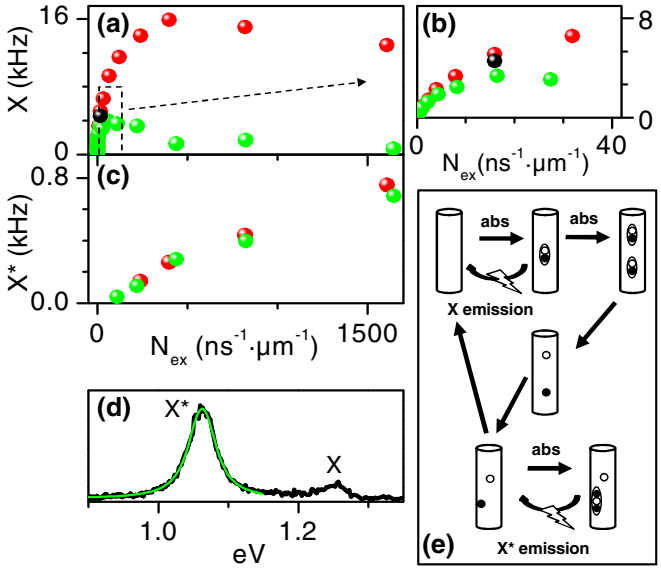

FIG. 3 (color online). (a) N_{ex} dependence of the X emission rate of an individual (6,5) nanotube excited at the S_{22} [light gray (green)] and at the phonon sideband [dark gray (red)]. (b) Zoom of (a) at low N_{ex}. (c) N_{ex} dependence of X^*. (d) Nanotube emission spectrum (black) recorded at $N_{ex} \sim 500$ ns$^{-1} \cdot \mu$m^{-1} (S_{22} excitation) fitted by a Lorentzian profile (green solid line). (e) Proposed mechanism for trion formation.

the S_{22} resonance, or at 1.47 eV [24], corresponding to the phonon sideband of the K-momentum exciton. In order to have a quantitative comparison between the two different excitation schemes, we carefully evaluated the number of prepared excitons N_{ex}, per unit time and unit length in both cases using published photophysical parameters [6,15].

In the spectra, X^* emission emerges from background at $N_{ex} \sim 100$ excitons μm$^{-1} \cdot$ ns^{-1}, which corresponds to a few (1–2) excitons present on average in a diffusion length ($\sim$ 100–200 nm, during an exciton lifetime of $\sim$100 ps [5,18]). This strongly indicates that the third carrier constituting the trion comes from a process of exciton-exciton interaction resulting in the annihilation of one exciton and the dissociation of the second one [Fig. 3(e)].

One key question is whether the photocreated charge carriers are freely diffusing along the SWCNT or localized. In the latter scenario, are these carriers trapped permanently or transiently present in the nanotubes?

At low N_{ex} (< 10 excitons ns$^{-1} \cdot \mu$m^{-1}) X exhibits a similar linear rise for the two excitation wavelengths; at higher N_{ex}, however, they differ drastically [Fig. 3(a)]. When excited near S_{22}, X emission is reproducible as long as the excitation remains sufficiently low. It reaches its maximum at $N_{ex} \sim 10$'s of excitons μm$^{-1} \cdot$ ns^{-1} before saturating and even decreasing irreversibly for higher exciton densities. When exciting at the phonon sideband, the X emission is reversible across the whole N_{ex} range studied here and reaches much higher rates before leveling off at greater N_{ex} (hundreds of excitons ns$^{-1} \cdot \mu$m^{-1}). In contrast, X^* keeps increasing for N_{ex} up to $\sim$1500 excitons μm$^{-1} \cdot$ ns^{-1}, and exhibits a similar evolution with N_{ex}, regardless of the excitation photon energy [Fig. 3(b)]. The saturation of X emission can have two different origins: EEA, which occurs on the $\sim$1 ps time scale for two excitons prepared in $\sim$0.4 μm nanotube segments [8,25], or diffusion limited contact-induced nonradiative relaxation of excitons at stationary quenching sites [5]. The former process is intrinsic and does not depend on the excitation wavelength [26] since the prepared excitons relax extremely rapidly down to the emitting state before interacting [27]. Thus, EEA cannot explain the observed difference in the N_{ex} dependence of X emission rates [Fig. 3(a)]. The latter, however, could depend on the excitation photon energy since the luminescence quenching sites can be laser induced [28]. Indeed, in comparison to excitation at the phonon sideband, S_{22} excitation presumably populates more photoreactive excitonic levels and thus produces a greater number of quenching sites [29] which dramatically degrade X emission. Accordingly, when returning to lower intensity after high illumination, the initial X count rate is not recovered (not shown) with S_{22} excitation in contrast to near-IR excitation [black symbol in Figs. 3(a) and 3(b)]. This indicates that the saturation behavior for excitation at the phonon sideband is mainly due to EEA while for S_{22} excitation it is dominated by laser-induced quenching sites.

The fact that, unlike X emission, X^* emission shows similar dependence on N_{ex}, regardless of the excitation wavelength, suggests that trion localization prevents their migration to photoinduced quenching sites. Trion localization is further supported by the Lorentzian shape of the X^* emission line [Fig. 3(d)]. Indeed, the recombination of a free trion would produce a free carrier and give rise to an asymmetric emission line with a tail towards the low photon energies due to the effective mass difference between the initial and final quasiparticles [30].

We conjecture that under high N_{ex} EEA creates charge carriers transiently trapped at electrostatic potential fluctuations [31] induced by inhomogeneities in the nanotube environment [32,33]. Subsequent photon absorption leads to trion formation consisting of an exciton bound to one of these localized carriers [Fig. 3(e)]. It is noteworthy that potential wells' spatial heterogeneities undergone by a single tube should have a negligible influence on the X^* line measured at room temperature since a trion and the charge carrier left over after its recombination are in the same potential wells. X^* transition energy variations should thus remain weaker than the observed linewidth. We also estimate that the contribution to ΔE of the charge's localization energy lies within our experimental precision ($\sim$ 5 meV).

To investigate the dynamics of these localized charge carriers that facilitate trion formation, we performed time-resolved pump-probe measurements on chirality-sorted (6,5) nanotube suspensions [15]. A regenerative

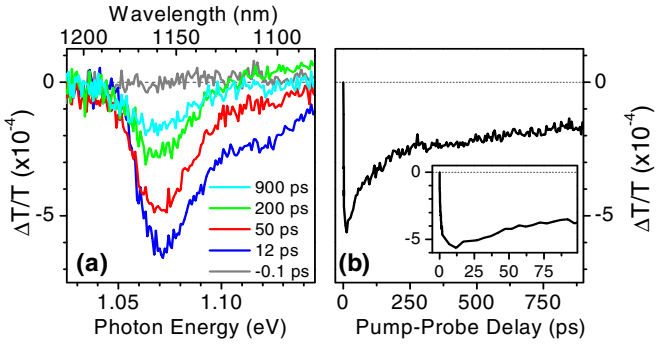

FIG. 4 (color online). Transient absorption spectra measured on (6,5) nanotubes at different pump-probe delays (pump resonant with X line) revealing a clear induced absorption at the X^* position. (b) Transient dynamics at 1.07 eV. Inset shows a zoom of short time delays.

Ti:sapphire amplifier (200 kHz repetition rate) followed by an optical parametric amplifier delivered femtosecond pump pulses (fluences between 5×10^{12} and 2.5×10^{14} photons per cm^2) resonant with S_{11}. Continuum probe pulses covering the X^* spectral range were generated in a sapphire crystal. Differential transmission spectra were acquired on a spectrometer-coupled InGaAs linear array as a function of the pump-probe time delay (~ 100 fs temporal resolution and down to a few 10^{-5} sensitivity).

In Fig. 4(a), a clear induced absorption (IA) feature is visible at the X^* position. The pump pulses generate multiple excitons in the SWCNTs which undergo fast EEA, resulting in the creation of a population of charge carriers that provide the third body for trion formation following absorption of probe photons at 1.07 eV [Fig. 3(e)]. The IA starts rising instantaneously after pump excitation and reaches its maximum within a few picoseconds [Fig. 4(b)]. This rise time is comparable to the first short decay time of the X population [34] due to EEA processes. The X^* IA decay time reflects the evanescence of the photogenerated charge carrier population within several hundreds of picoseconds. For trion formation to occur, photoinduced charge carriers must spatially separate and should thus be localized to avoid their spatial overlap and further recombination. The dynamics observed in Fig. 4(b) would then reflect the creation and trapping of the charge carriers (IA rise) and their untrapping (IA decay). The fairly slow IA relaxation further supports the scenario in which the charge carriers are localized. After a few hundreds of picoseconds, trion IA spectra are symmetric [Fig. 4(a)]. This is consistent with the symmetric X^* luminescence spectra [Fig. 3(d)]. The asymmetry observed at short pump-probe delays is due to a superposition of a faster transient signal centered near 1.13 eV whose origin can be attributed to contributions from other fast many-body effects. A detailed analysis of the transient absorption spectra will be published elsewhere.

Importantly, the existence of a transient signal at positive delays and its absence at negative delays demonstrates that the carriers that allow trion formation are indeed photogenerated and not present permanently in the SWCNTs.

In conclusion, we have shown trion emission in pristine carbon nanotubes. Investigations of trion photophysics in various media and temperature conditions could be used as a probe of electrostatic environment, a key parameter for applications of carbon nanotubes in photonic and optoelectronic devices. This work opens the possibility of all-optical manipulation of electron or hole spins in SWCNTs for quantum information [35].

We thank R. B. Weisman and S. Ghosh for supplying us with the DGU samples and critical reading of the manuscript, J. Besbas for experimental help, and B. Hönerlage for helpful discussions. This work was funded by ANR, ERC, and Région Aquitaine. J. S. acknowledges support from the W. J. Fulbright Commission.

*Corresponding author.
blounis@u-bordeaux1.fr

[1] F. Wang *et al.*, Science **308**, 838 (2005).
[2] J. Maultzsch *et al.*, Phys. Rev. B **72**, 241402(R) (2005).
[3] A. Jorio, G. Dresselhaus, and M. S. Dresselhaus, *Carbon Nanotubes* (Springer, Berlin, 2008).
[4] A. Hagen *et al.*, Phys. Rev. Lett. **95**, 197401 (2005).
[5] L. Cognet *et al.*, Science **316**, 1465 (2007).
[6] S. Berciaud, L. Cognet, and B. Lounis, Phys. Rev. Lett. **101**, 077402 (2008).
[7] J. Lefebvre *et al.*, Nano Lett. **6**, 1603 (2006).
[8] Y. Z. Ma *et al.*, Phys. Rev. Lett. **94**, 157402 (2005).
[9] F. Wang *et al.*, Phys. Rev. Lett.**92**, 177401 (2004).
[10] T. G. Pedersen *et al.*, Nano Lett. **5**, 291 (2005).
[11] D. Kammerlander *et al.*, Phys. Rev. Lett. **99**, 126806 (2007).
[12] K. Watanabe and K. Asano, Phys. Rev. B **83**, 115406 (2011).
[13] T. F. Rønnow, T. G. Pedersen, and H. D. Cornean, Phys. Rev. B **81**, 205446 (2010).
[14] R. Matsunaga, K. Matsuda, and Y. Kanemitsu, Phys. Rev. Lett. **106**, 037404 (2011).
[15] S. Ghosh, S. M. Bachilo, and R. B. Weisman, Nature Nanotech. **5**, 443 (2010).
[16] O. N. Torrens, M. Zheng, and J. M. Kikkawa, Phys. Rev. Lett. **101**, 157401 (2008).
[17] Y. Murakami *et al.*, Phys. Rev. B **79**, 195407 (2009).
[18] T. Gokus *et al.*, J. Phys. Chem. C **114**, 14 025 (2010).
[19] R. Matsunaga, K. Matsuda, and Y. Kanemitsu, Phys. Rev. B **81**, 033401 (2010).
[20] H. Harutyunyan *et al.*, Nano Lett. **9**, 2010 (2009).
[21] K. Nagatsu *et al.*, Phys. Rev. Lett. **105**, 157403 (2010).
[22] S. Ghosh *et al.*, Science **330**, 1656 (2010).
[23] R. B. Capaz *et al.*, Phys. Status Solidi B **244**, 4016 (2007).
[24] S. Berciaud *et al.*, Nano Lett. **7**, 1203 (2007).
[25] F. Wang *et al.*, Phys. Rev. B **70**, 241403(R) (2004).
[26] Y. Murakami and J. Kono, Phys. Rev. B **80**, 035432 (2009).
[27] C. Manzoni *et al.*, Phys. Rev. Lett. **94**, 207401 (2005).

[28] C. Georgi *et al.*, Chem. Phys. Chem. **9**, 1460 (2008).
[29] J. L. Blackburn *et al.*, Nano Lett. **8**, 1047 (2008).
[30] J. B. Grun *et al.*, *Physics of Highly Excited States in Solids* (Springer-Verlag, Berlin, 1976).
[31] D. Brinkmann *et al.*, Phys. Rev. B **60**, 4474 (1999).
[32] A. Hogele *et al.*, Phys. Rev. Lett. **100**, 217401 (2008).
[33] V. Perebeinos and P. Avouris, Phys. Rev. Lett. **101**, 057401 (2008).
[34] L. Luer *et al.*, Nature Phys. **5**, 54 (2008).
[35] C. Galland and A. Imamoglu, Phys. Rev. Lett. **101**, 157404 (2008).